NORWEGIAN JOURNAL OF GEOLOGY
https://dx.doi.org/10.17850/njg103-2-3

GEOLOGICAL SOCIETY OF NORWAY

Detrital zircons of the vast Triassic Snadd and De Geerdalen formations, Barents Shelf, reveal temporal changes in sediment source

Trond Svånå Harstad[1, 4], Trond Slagstad[2], Christopher L. Kirkland[3] & Mai Britt E. Mørk[1]

[1]*Department of Geoscience and Petroleum, Norwegian University of Science and Technology (NTNU) S. P. Andersens veg 15a, 7031 Trondheim, Norway*
[2] *Geological Survey of Norway, Postbox 6315, Torgarden 7491 Trondheim, Norway*
[3]*Timescales of Mineral Systems Group, School of Earth and Planetary Sciences, Curtin University, Perth, Western Australia 6102, Australia.*
[4]*Current address: Exploro Geoservices, Innherredsveien 7, 7014 Trondheim*

E-mail corresponding author (Trond Svanå Harstad) trondsh@gmail.com

Keywords:
- *Detrial zircon*
- *Geochronology*
- *Provenance*
- *Snadd Formation*
- *Triassic*
- *Barents Sea*
- *Sverdrup Basin*

Electronic supplement 1:
Supplement A:
Zircon U–Pb age dataset.

Electronic supplement 2:
Supplement B:
Zircon Lu–Hf isotope dataset.

Received:
18. May 2022

Accepted:
20. April 2023

Published online:
10. November 2023

Studies of detrital-zircon age distributions from Triassic sedimentary rock successions on the Arctic Barents Shelf have resulted in different provenance interpretations. Here, we provide new U–Pb/Hf detrital-zircon data from eleven samples of the Snadd and De Geerdalen formations, covering the Barents Shelf in a north–south transect, that help refine the provenance of these sedimentary rocks and show how stratigraphic variations reflect changing source regions. The sample locations cover different stratigraphic levels and geographic locations within the formations. The detrital-zircon age spectra in the lower part (lowest Ladinian and lower Carnian) are dominated by two age peaks at 300 and 540 Ma, whereas the zircon distributions in the stratigraphically younger deposits (latest Carnian and early Norian) are dominated by a 235 Ma age peak and two minor peaks at 300 and 425 Ma. The apparent relative contribution of detritus of different ages changes gradually from lower to higher stratigraphic levels, marked by an increase in both the 235 and 425 Ma age peaks, a decrease in the 300 Ma component and a progressive loss of the 540 Ma age peak. The zircon Hf-isotopic compositions display predominantly juvenile zircon populations, except for a mixed juvenile and evolved signature in the youngest Permo-Triassic grains. A regional comparison of detrital-zircon age spectra in latest Carnian/early Norian deposits extends the depositional system into the Sverdrup Basin, supporting a much larger depositional system than hitherto known. The gradual change in detrital-zircon age spectra likely represents a gradual shift in zircon provenance. We interpret these variations to reflect an early source region in the north Urals, gradually changing to a dominant source region in the Taimyr Peninsula region.

Harstad, T.S., Slagstad, T., Kirikland, C.L. & Mørk, M.B. 2023: Detrital zircons of the vast Triassic Snadd and De Geerdalen formations, Barents Shelf, reveal temporal changes in sediment source. *Norwegian Journal of Geology 103*, 202308. https://dx.doi.org/10.17850/njg103-2-3

Introduction

Extensive Triassic sedimentary rocks in the Arctic region have detrital-zircon cargos dominated by Ediacaran to Triassic ages (Miller et al., 2006, 2013; Omma et al., 2011; Tuchkova et al., 2011; Pózer Bue & Andresen, 2014; Letnikova et al., 2014; Soloviev et al., 2015; Fleming et al., 2016; Midwinter et al., 2016; Zhang et al., 2016; 2018b; Flowerdew et al., 2019; Khudoley et al., 2019). The late Palaeozoic Uralian Orogen (mostly active 400–300 Ma), located east of the Barents Basin (Fig. 1), has traditionally been considered the source of these grains (e.g., Miller et al., 2013); however, different interpretations have been proposed to account for the variations in detrital-zircon age components. In particular, it is unclear if a Uralian Orogen source can account for the youngest detrital-zircon populations and whether coeval sediments in the Sverdrup Basin, east of the Barents Basin, were derived from the same easterly source area (Klausen et al., 2015; Fleming et al., 2016; Midwinter et al., 2016; Gilmulina et al., 2022). Upper Triassic deposits have distinct populations of Triassic zircon (Omma et al., 2011; Tuchkova et al., 2011; Pózer Bue & Andresen, 2014; Letnikova et al., 2014; Soloviev et al., 2015; Fleming et al., 2016; Midwinter et al., 2016; Klausen et al., 2017; Flowerdew et al., 2019), which challenges the interpretation of a sole Uralian Orogen source because activity in the Uralian Orogen is now known to have ceased in the Permian (Puchkov, 2009; Klausen et al., 2015; Vernikovsky et al., 2020; Harstad et al., 2021). The provenance of the Late Triassic Sverdrup Basin deposits has also been the topic of different interpretations, one favouring a Uralian Orogen source while another suggests derivation from an island-arc terrane that lay to the north of the Sverdrup Basin (Omma et al., 2011; Midwinter et al., 2016, Anfinson et al., 2016; Hadlari et al., 2018).

New research into the tectonic evolution in the Arctic region helps to identify two important events that potentially explain a Triassic zircon source, namely tectonism in the Novaya Zemlya–Kara Sea and Taimyr regions (Fleming et al., 2016; Klausen et al., 2017; Zhang et al., 2018a; 2018b) and the Siberian Traps large igneous province (LIP) (Zhang et al., 2016). Geographically controlled, intra-formational variation in detrital-zircon age spectra has also been documented, suggesting that different parts of this extensive, Triassic depositional system may have been fed by different river systems sampling different sources (Fleming et al., 2016). Flemming et al. (2016) suggested that sediments off the northern margin of Norway were derived from a Caledonian source, whereas sediments farther north on the Barents Shelf were derived from either South Uralian (The greater Ural – mountains region) or North Uralian (the present day Pai- Koi, Novaya Zemlya and Taimyr region) sources.

In this contribution, we present detrital-zircon U–Pb and Lu–Hf data from the Middle- to Upper Triassic Snadd- and De Geerdalen formations on the Barents Shelf, generally interpreted to have been derived from Uralian sources, as defined by Flemming et al. (2016). Our new data come from various intra-formational stratigraphic positions and locations not previously analysed to help refine the general geological understanding of a Uralian source. This work questions the validity of contemporaneous South- and North Uralian sources. Instead, these new data suggest that different sediment sources may have been dominant at different times, most likely due to tectonic events in the source regions. We further show that this depositional system was much more widespread than the Barents Sea area, most likely also including the distant Sverdrup Basin, thus adding important new knowledge about what is arguably the largest known delta depositional system in the world (Klausen et al., 2019; Gilmulina et al., 2021).

Ediacaran to Triassic Arctic geological evolution

The Ediacaran to Triassic evolution of the Barents Sea region (including Arctic Russia, Scandinavia and Greenland) is characterised by several key tectonic events influencing the development and provenance signatures of the Barents Shelf (Fig. 1). The Archaean through Proterozoic cratons of Siberia, Baltica and Laurentia likely represented independent continents in the late Neoproterozoic, after break-up of the supercontinent Rodinia (Cocks & Torsvik, 2007, 2011; Nystuen et al., 2008; Willner et al., 2019). Siberia and Baltica may have been located close to each other, at a distance from Laurentia (Priyatkina et al., 2017). This configuration changed in the Phanerozoic, with collision between Laurentia and Baltica in the Siluro-Devonian Caledonian Orogeny. The later Devonian to Permian collision between Baltica, Kazakhstania and Siberia in the Uralian Orogeny represents the final amalgamation of the northern part of Pangea (Puchkov, 2009; Nikishin et al., 2010; Vernikovsky et al., 2020). Extensive volcanism associated with the formation of the 250 Ma Siberian Traps LIP on the Siberian Craton marked the transition into the Mesozoic Era (Reichow et al., 2009; Ivanov et al., 2018).

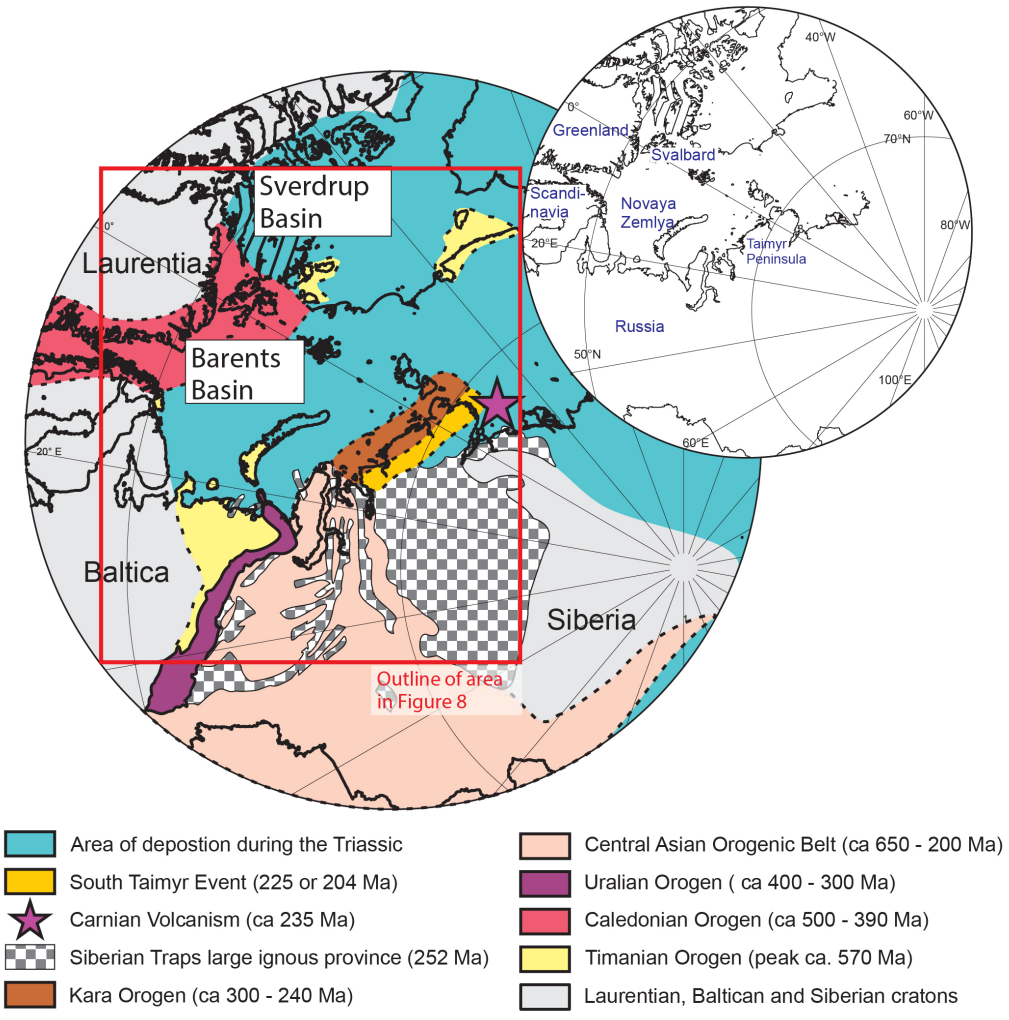

Figure 1. Palaeogeographic reconstruction of the polar areas in the Late Triassic showing areas of several major tectonic events of the Neoproterozoic to Late Triassic, major areas of Triassic deposition and regional locations. As the figure represents an extended period, the considerable overlap between units is not accounted for in the figure. Late Triassic palaeogeography, extent of depositional and offshore areas modified after Sømme et al. (2018). Outline of the Timanian and Caledonian Orogens after Gee et al. (2006), Willner et al. (2019) and Ershova et al. (2016), outline of the present-day Ural mountains after Puchkov (2009), outline of the Central Asian Orogenic Belt after Xiao et al. (2015) and Ershova et al. (2016), outline of the Siberian Traps large igneous province after Ivanov et al. (2018) and the outline of the Kara Orogen after Vernikovsky et al. (2020). The South Taimyr event is suggested based on Zhang et al. (2018a). Possible location of Carnian volcanic activity based on Letnikova et al. (2014) and references therein.

Neoproterozoic tectonic events

Few large-scale tectonic events impacted Baltica and Greenland in the Neoproterozoic until continental breakup and plate divergence around 615 Ma (Nystuen et al., 2008). Simultaneous with Baltica–Laurentia break-up, a collisional regime was present in the northeastern part of Baltica, in the Timanian Orogen (Fig. 1; Gee et al., 2006; Kuznetsov et al., 2007; Willner et al., 2019). The Timanian Orogen resulted in metamorphism of passive-margin sedimentary rocks and magmatic activity in an accretionary tectonic setting that peaked between 580 and 550 Ma (Olovyanishnikov et al., 2000; Gee & Pease, 2004), but may have lasted from 700 to 515 Ma (Kuznetsov et al., 2007). Detrital zircon of Timanian age is predominant in Cambro-Silurian successions in the Novaya Zemlya and Severnaya Zemlya archipelagos (Lorenz et al., 2008, 2013), and these sediments were likely more widely distributed. The Neoproterozoic Taimyr Orogen, located on the Taimyr Peninsula (Fig. 1), represents a Neoproterozoic accretionary orogen north of the Siberian craton (Priyatkina et al., 2017). Magmatic zircon was produced during two accretionary phases, first at 900–800 Ma related to continental-arc magmatism and at 750–600 Ma in a back-arc to continental-arc setting (Priyatkina et al., 2017). The latter event may have been linked to the Timanian Orogen (Priyatkina et al., 2017).

Palaeozoic tectonic events

Two Phanerozoic collisional orogenies affected the region: the Caledonian and Uralian (Fig. 1). The Caledonian Orogen covered a large area of what is now East Greenland – western Scandinavia, Svalbard and the Barents Sea (Gee et al., 2006; Corfu et al., 2014). Zircons derived from the Caledonian Orogen typically range in age between 500 and 390 Ma and are commonly accompanied by large populations of Mesoproterozoic grains (Bingen & Solli, 2009; Pózer Bue & Andresen, 2014). Caledonian syn- and post-collisional sedimentary rocks, especially Devonian Old Red Sandstones, are present in large areas of the Arctic (Dineley, 1975; Lorenz et al., 2008; 2013), making them likely candidates for later erosion and re-sedimentation.

Detrital-zircon populations from the Uralian Orogen are characterised by Late Devonian to Permian ages (Pózer Bue & Andresen, 2014; Fleming et al., 2016). The Uralian Orogen comprises stacked units of foreland sedimentary rocks, pre-Uralian passive-margin sedimentary rocks, pre-collisional continental rocks, several ophiolites, island-arc terranes and granitic intrusive belts (Puchkov, 2009). The Uralian Orogen is sometimes considered part of the larger Central Asian Orogenic Belt (CAOB) (Xiao et al., 2015; Ershova et al., 2016), which consists of several Neoproterozoic microcontinent- and island-arc terranes that amalgamated with Siberia/Baltica in the Permo-Triassic (Xiao et al., 2015). Detrital zircon derived from the CAOB is described from voluminous Permian deposits on the Verkhoyansk passive margin on the northern and eastern parts of the Siberian Craton, including south Taimyr (Ershova et al., 2016). The detrital-zircon age distributions in these deposits have noticeable peaks in the Permian, Carboniferous, Cambrian (500 Ma) and the Neoproterozoic (750–850 Ma) (Ershova et al., 2016).

Triassic regional development

The timing and tectonic significance of Permo–Triassic events in the Taimyr, Severnaya Zemlya, Kara Sea and Novaya Zemlya region (Fig. 1) remain enigmatic, although several recent scientific contributions have shed light on the topic (Zhang et al., 2016; 2018a; 2018b; Khudoley et al., 2018; Vernikovsky et al., 2020). In North Taimyr, the Siberian craton collided with the Kara Terrane resulting in the Permian to Middle Triassic Kara Orogeny (Vernikovsky et al., 2020). Deformation is documented in South Taimyr in the Late Triassic (225 Ma; Zhang et al., 2016; 2018a) or possibly latest Triassic–Early

Jurassic (Khudoley et al., 2018) and resulted in substantial amounts of crustal shortening (Zhang et al., 2018a). Deformation and erosion on Novaya Zemlya are also documented in the Late Triassic at around 210 Ma (Zhang et al., 2018b).

At the Permo-Triassic boundary, formation of the Siberian Traps LIP involved extrusion of large volumes of mostly mafic volcanic material in Siberia (Reichow et al., 2009). The active phase of volcanism seems to have been restricted to approximately three million years, around 250 Ma (Reichow et al., 2009). Younger Triassic igneous rocks have been documented in northern Siberia in recent years (Letnikova et al., 2014; Ivanov et al., 2018; Vernikovsky et al., 2020), of which trachytic volcanic rocks in the Carnian Osipai Formation in the Lena delta area represent the largest volumes (Letnikova et al., 2014 and references therein). Several researchers have suggested that Middle and Late Triassic magmatism represents a late-stage continuation of the Siberian Traps LIP (Letnikova et al., 2014; Zhang et al., 2016; Vernikovsky et al., 2020).

The Triassic Barents Shelf

In the Early Triassic, the Barents Shelf was a 1.3 million km^2 basin in the Boreal Sea, north of Pangea (Pózer Bue & Andresen, 2014; Klausen et al., 2015; Sømme et al., 2018). In the Lower Triassic succession, there were several proximal depositional systems in and around the basin, as documented proximal to the Baltican Shield and Greenland (e.g., Eide et al., 2018). The predominant sediment source seems, however, to be the Uralian Orogen, with a sediment influx prograding from the southeast (all directions refer to present day) (Mørk, 1999; Riis et al., 2008; Glørstad-Clark et al., 2010; Henriksen et al., 2011; Lundschien et al., 2014; Klausen et al., 2015, 2019; Sømme et al., 2018; Harstad et al., 2021). Continuous sediment supply from the east-southeast eventually led to a complete infilling of the basin (Lundschien et al., 2014; Klausen et al., 2015, 2019). Deposition of the marginal-marine to fluvial Snadd and De Geerdalen formations – the topic of this contribution – during the Ladinian to lower Norian is considered the final stage in this evolution (Klausen et al., 2015, 2019). The northerly derived Pat Bay Formation in the Sverdrup Basin potentially represents the farthest known extent of this system (Omma et al., 2011), although this interpretation remains disputed (Midwinter et al., 2016; Gilmullina et al., 2022). In the latest Triassic, parts of the region developed an erosional relief (Klausen et al., 2017).

Previous work on the sedimentology and provenance of the Snadd and De Geerdalen formations

The Snadd and De Geerdalen sandstones are mineralogically immature arkosic to lithic arenites, with the exception of mature sandstones in the southern Hammerfest Basin (Mørk, 1999, 2013; Fleming et al., 2016). The immature sandstones have relatively low quartz and K-feldspar content and comparatively high concentrations of plagioclase and rock fragments (Mørk, 1999, 2013; Fleming et al., 2016). The presence of volcanic, mica schist and biogenic rock fragments (Mørk et al., 1982; Mørk, 1999; 2013; Soloviev et al., 2015), along with higher concentrations of the stable heavy minerals (Morton & Hallsworth, 1999; Mørk, 1999; Fleming et al., 2016; Flowerdew et al., 2019), point to sedimentary, metasedimentary and volcanic source rocks. Sizable heavy-mineral populations of apatite, chloritoid, Cr-spinel, garnet, titanite, tourmaline and zircon are reported in the formations; these are minerals that typically form in metamorphic and igneous rocks (Mørk, 1999; Fleming et al., 2016).

Published research on the provenance of the Snadd and/or De Geerdalen formations mainly follows one of two methodologies. One approach is based on sedimentological and stratigraphic analysis and focuses on seismic-scale features (Riis et al., 2008; Glørstad-Clark et al., 2010; Høy & Lundschien, 2011; Lundschien et al., 2014; Klausen et al., 2015; Gilmullina et al., 2021) and field observations from Svalbard (Mørk et al., 1982; Høy & Lundschien, 2011). The second approach emphasises petrographic and mineral observations, and in particular single-grain geochronology and chemistry (Bergan & Knarud, 1993; Mørk, 1999, 2013; Muller & Knies, 2013; Pózer Bue & Andresen, 2014; Soloviev et al., 2015; Fleming et al., 2016; Flowerdew et al., 2019; Harstad et al., 2021).

Seismicity-based research interprets the Snadd and De Geerdalen-formation sedimentary rocks to be deposited in mappable, large-scale clinoforms prograding from the southeast in a northwest direction (Riis et al,. 2008; Glørstad-Clark et al., 2010; Lundschien et al., 2014; Klausen et al., 2015), supported by palaeocurrent measurements from Svalbard (Høy & Lundschien, 2011). The most likely source of these sediments is the Uralian Orogen (Riis et al,. 2008; Glørstad-Clark et al., 2010; Lundschien et al., 2014; Klausen et al., 2015), inferred from the transport direction and original proximity to the Uralian mountain belt. A second, much less voluminous Greenland sediment source is reported on the western margin of the basin, supported by palaeocurrent observations on western Svalbard (Mørk et al., 1982) and seismic sections along the western shelf margin (Glørstad-Clark et al., 2010).

Petrographic and geochronological, single-grain provenance methods have generally also favoured a Uralian Orogen provenance, in addition to more local sources near the Baltic Shield (Mørk, 1999; Pózer Bue & Andresen, 2014; Soloviev et al., 2015; Fleming et al., 2016; Flowerdew et al., 2019; Harstad et al., 2021).

Published detrital-zircon age distributions from Svalbard (Pózer Bue & Andresen, 2014), Franz Josef Land (Soloviev et al., 2015; Khudoley et al., 2019) and the southern Barents Sea (Fleming et al., 2016; Flowerdew et al., 2019; Line et al., 2020) show zircon populations mostly in the age range 600–225 Ma. This age range is distinctly different from zircon populations in sediments derived from Greenland and Baltica (Pózer Bue & Andresen, 2014). Key zircon age peaks are observed from various locations and stratigraphic levels within the Snadd and De Geerdalen formations and include a dominant peak at 300 Ma, several small peaks in the range 400–300 Ma, and a minor peak at 550 Ma that is characteristic for samples from the southern Barents Sea (Fleming et al., 2016). Published zircon age spectra from locations on the northern Barents Shelf show a somewhat different pattern with dominant age peaks at 235, 300 and 420 Ma (Pózer Bue & Andresen, 2014; Soloviev et al., 2015). Detrital zircon age spectra variations within the Snadd and De Geerdalen formations have been attributed to geographical variations in provenance (Fleming et al., 2016), including a North Uralian provenance on Svalbard and Franz Josef Land and a South Uralian provenance on the southern Barents Shelf (Fleming et al., 2016). Flowerdew et al. (2019) discussed the possibility of a potential mixed source, with recently eroded material and recycled Uralian Orogen detritus, that accounts for apparent similarities between these sources.

Other single-grain chemical and/or geochronological methods have generally supported a Uralian Orogen provenance for the Snadd and De Geerdalen formations. Flowerdew et al. (2019) describe detrital-apatite age distributions similar to the detrital-zircon age distributions. Harstad et al. (2021) investigated detrital Cr-spinel compositions on the same samples as those discussed in this contribution and concluded that a similar, uniform source of detrital Cr-spinel was likely for all samples. They advocated a metamorphosed ophiolitic ultramafic complex as the ultimate source for the Cr-spinel in the investigated samples and tied this source to the Uralian Orogen. This source is distinctly different from contemporaneous Siberian Traps LIP-related detrital Cr-spinel in Siberia (Nikolenko et al., 2018).

Sampling

This study is based on detrital-zircon U–Pb and Lu–Hf data from 11 samples in a SE–NW transect across the Norwegian Barents Shelf (Fig. 2, Table 1). Sample details are presented in Table 1; see Harstad et al. (2021) for further sample details and a discussion of the Cr-spinel data. All samples were collected from sandstones within the Snadd Formation on the Barents Sea Shelf and the equivalent De Geerdalen Formation onshore Svalbard and represent parts of a prograding delta succession deposited in barrier, shoreface, marginal-marine and delta-plain environments (Bugge et al., 2002; Riis et al., 2008; Stensland et al., 2013; Lundschien et al., 2014; Vigran et al., 2014). Different clinoforms (e.g., Klausen et al., 2015) are represented in the sample material and the stratigraphy follows that proposed by Bugge et al. (2002), Lundschien et al. (2014) and Vigran et al. (2014). Sample locations include the Nordkapp

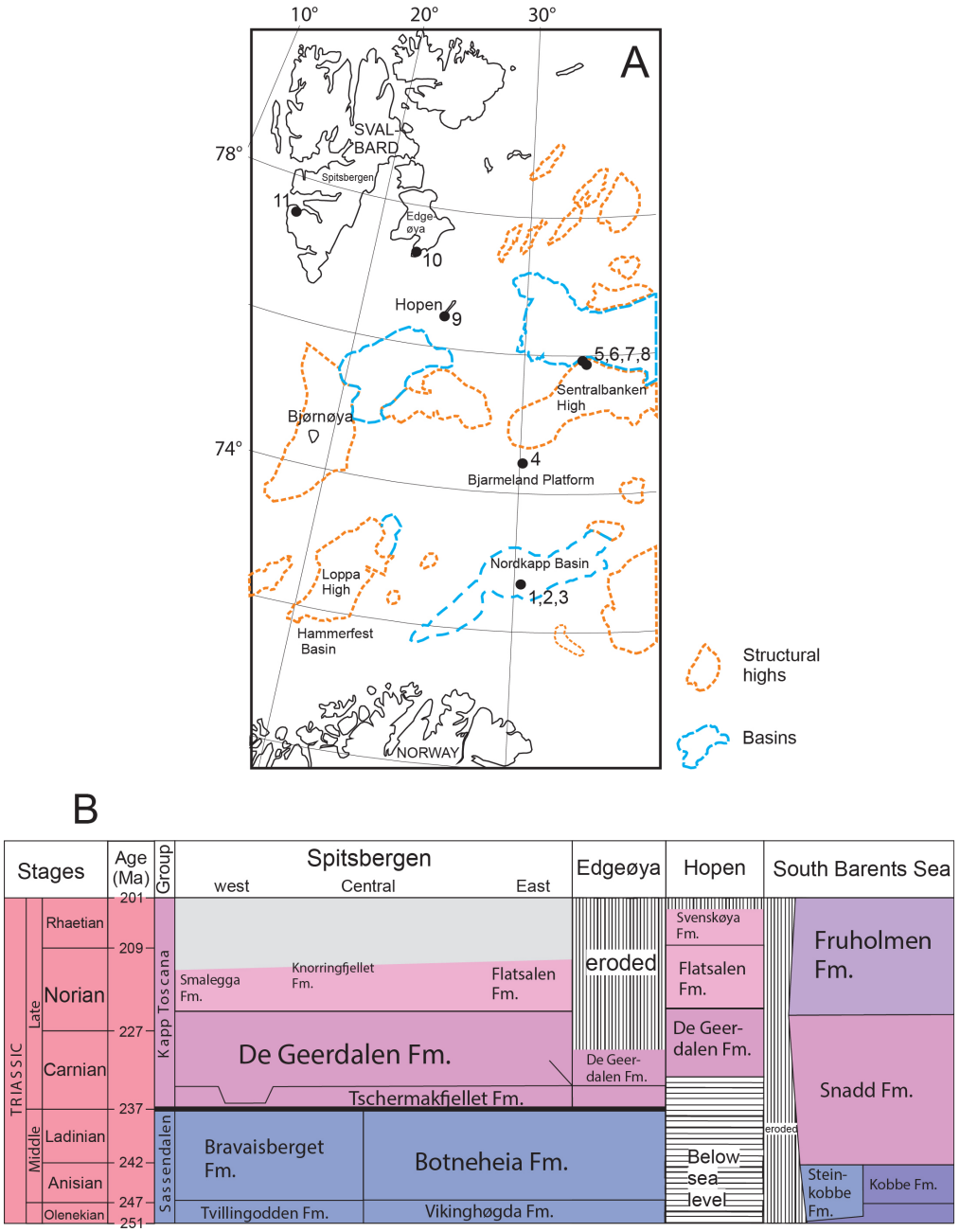

Figure 2. (A) Map of the Norwegian Barents Shelf with outlines of structural highs and basins, modified from Lundschien et al., 2014. Sample locations are indicated with black spots and numbered as in Table 1. (B) Lithostratigraphic overview of the Triassic of the sampled area (Lundschien et al., 2014).

Table 1. An overview of studied samples including number of analysed zircon grains. Sample 1–8 are Snadd Fm. samples, sample 9–11 are from the De Geerdalen Fm. Sample numbers are arranged geographically; Southeast (1) to Northwest (11). Stratigraphic age based on biostratigraphic ages in Bugge et al. (2002), and Vigran et al. (2014), while Lundschien et al. (2014), and Klausen et al. (2015) add lithostratigraphic correlations to the interpretations.

Area and Formation		Stratigraphic age	Well number/ Field sample	East	North	**Sample ID in text**	Depth below seafloor	No. of analysed zircons	No. of analyses <10% discordant
Barents Sea Snadd Fm.	Nordkapp Basin	Late Carnian	7230/05-U-03	30° 22' 26.7'' E	72° 41' 10.05'' N	**1**	114 m	129	78
		Ladinian	7230/05-U-05	30° 22' 31.64'' E	72° 42' 6'' N	**2**	33 m	115	82
			7230/05-U-05	30° 22' 31.64'' E	72° 42' 6'' N	**3**	38 m	148	93
	Bjarmeland Platform	Middle Carnian	7430/07-U-01	30° 14' 56.145'' E	74° 26' 34.703''N	**4**	56 m	149	125
	Sentral-banken High	Early Carnian	7533/02-U-01	33° 25' 37.6'' E	75° 55' 41.93'' N	**5**	46 m	113	76
			7533/02-U-01	33° 25' 37.6'' E	75° 55' 41.93'' N	**6**	123 m	200	144
			7533/03-U-07	33° 55' 22.24'' E	75° 48' 27.65'' N	**7**	111 m	184	129
			7533/03-U-07	33° 55' 22.24'' E	75° 48' 27.65'' N	**8**	147 m	60	40
Svalbard De Geerdalen Fm.	Hopen	Late Carnian	H30	UTM35 446533	8487870	**9**		221	144
	Edgeøya	Late Carnian	EO25	UTM35 395946	8585416	**10**		211	134
	West Spitsbergen	Late Carnian/ Norian (?)	KTO12 + KTO14	UTM33 501340	8608640	**11**		189	140

Basin, Bjarmeland Platform and Sentralbanken High in the Barents Sea, and Hopen, Edgeøya and West Spitsbergen (van Koelenfjorden) onshore Svalbard. The offshore Snadd Formation samples are from shallow stratigraphic cores drilled by IKU (SINTEF Petroleum) and the Norwegian Petroleum Directorate (NPD) (Bugge et al., 2002; Lundschien et al., 2014). Onshore samples of De Geerdalen Formation sandstones were collected during a SINTEF- and NPD-led expedition in August 2014. Ladinian and uppermost Carnian deposits are sampled from shallow cores in the Nordkapp Basin, lower Carnian at the Sentralbanken High, and middle Carnian deposits in the Bjarmeland Platform area. The samples collected from outcrops on Svalbard represent upper Carnian and possibly lowermost Norian deposits.

The studied samples represent well-sorted, fine- and medium-grained sandstones, and are from units described in the literature as mineralogically immature lithic and arkosic arenites (Mørk, 1999, 2013; Riis et al., 2008). The main detrital components are quartz, K-feldspar, plagioclase, mica, abundant cherty rock fragments, as well as lithic clasts of altered volcanic/igneous, metamorphic and recycled sedimentary rocks. Common accessory heavy minerals in the formations include Cr-spinel, zircon, garnet, tourmaline and opaque minerals (Mørk, 1999, 2013; Harstad et al., 2021).

Methods

The collected samples were crushed and dry-sieved to obtain the 37–250 µm fraction. Zircon was separated from the sand fraction by heavy-liquid (diiodmethane, 3.325 g/mL) separation and hand-picked with tweezers under a binocular microscope. Grains were mounted in epoxy and polished to expose their interiors. A 1450VP Scanning Electron Microscope (SEM) from LEO Electron Microscopy LTD at the Geological Survey of Norway (NGU), Trondheim, was used to obtain back-scatter electron and cathodoluminescence (CL) images.

At NGU, an Element XR single-collector, high-resolution ICP–MS coupled to a New Wave Research UP193–FX nm short-pulse excimer laser-ablation system was used to measure U–Pb isotopes in zircon. The laser ablated lines up to 60 µm with a spot size of 15 µm, a speed of 2 µm/s, a repetition rate of 10 Hz and an energy fluence of 3–4 J/cm^2. Background measurement for 29 s was followed by 30 s of ablation with measurements of the following isotopes: ^{202}Hg, ^{204}Pb, ^{206}Pb, ^{207}Pb, ^{208}Pb, ^{232}Th and ^{238}U. Analyses with high common lead were excluded from further calculations based on the ^{204}Pb measurements. The natural zircon reference material GJ–1 (608.5 ± 1.5 Ma; Jackson et al., 2004) was applied as a primary standard. Natural zircon material Plešovice (Sláma et al., 2008), 91500 (Wiedenbeck et al., 1995), OS-99-14 (Skår, 2002), Temora (Black et al., 2003) and Z-6412 (unpublished) were routinely analysed to assess data reliability. U–Th–Pb isotope ratios were calculated using Glitter (Van Actherbergh, 2001).

At Curtin University, zircon crystals were analysed using a split–stream laser ablation system where a portion of the ablated material was divided between a quadrupole ICP–MS for U–Pb analysis and a multi-collector ICPMS for Lu–Hf analysis. Zircon was ablated using a Resonetics RESOlution M–50A–LR system, incorporating a COMPex 102 193 nm excimer UV laser. Following two cleaning pulses and a 40 s period of background analysis, samples were spot ablated for 35 s at a 10 Hz repetition rate using a 50 µm beam and laser energy at the sample surface of 2.2 J/cm^2. An additional 40 s of baseline was collected after ablation. The sample cell was flushed with ultrahigh purity He (300 mL/min) and N_2 (1.0 mL/min) and high purity Ar was employed as the plasma carrier gas.

U–Pb isotopes were measured using an Agilent 7700s quadrupole ICP–MS, with high-purity Ar as the plasma gas (flow rate 0.98 L min−1) and GJ-1 (601.7 ± 1.4 Ma; Jackson et al., 2004) as the primary reference material, with 91500 (1062.4 ± 0.4 Ma; Wiedenbeck et al., 1995) and Plešovice (337.13 ± 0.37 Ma; Sláma et al., 2008) as secondary standards. ^{206}Pb/^{238}U ages calculated for all zircon age standards, treated as unknowns, were found to be within 3% of the accepted value.

The split for Lu–Hf analysis was measured on a Nu Plasma II multi-collector ICP–MS. All isotopes (^{180}Hf, ^{179}Hf, ^{178}Hf, ^{177}Hf, ^{176}Hf, ^{175}Lu, ^{174}Hf, ^{173}Yb, ^{172}Yb and ^{171}Yb) were counted on the Faraday collector array. Time–resolved data were baseline subtracted and reduced using Iolite (DRS after Woodhead et al., 2004), where ^{176}Yb and ^{176}Lu were removed from the 176 mass signal using ^{176}Yb/^{173}Yb = 0.7962 and ^{176}Lu/^{175}Lu = 0.02655 with an exponential law mass bias

correction assuming $^{172}Yb/^{173}Yb$ = 1.35274 (Chu et al., 2002). The interference corrected $^{176}Hf/^{177}Hf$ was normalised to $^{179}Hf/^{177}Hf$ = 0.7325 (Patchett & Tatsumoto, 1980) for mass bias correction. Zircon crystals from the Mud Tank carbonatite locality were analysed together with the samples in each session to monitor the accuracy of the results.

The $^{207}Pb/^{206}Pb$ age is used for zircons older than 1000 Ma, while the $^{206}Pb/^{238}U$ age is used for younger zircon grains. The U–Pb and Lu–Hf data are presented using the detzrcr R application (Andersen et al., 2018). All zircon data are provided in Electronic Supplements 1 and 2.

Results

A total of 1428 U–Pb isotope analyses were performed at NGU. In addition, 291 U–Pb and Lu–Hf analyses were performed at Curtin University. Forty-five of the zircon grains were first analysed for U and Pb at NGU, and then re-analysed for Lu and Hf isotopes at Curtin University. In total, 1719 zircon grains were dated, of which 1185 grains were less than 10% discordant and used to construct age probability density plots. A total of 113 Lu–Hf analyses are within the accepted discordance range; 45 analyses specifically targeted the youngest zircon grains. Zircon grain shape, colour and internal textures vary and the youngest grains are generally angular and/or euhedral and display oscillatory growth zoning.

Detrital zircon U–Pb age data

The data are presented according to geographic/geological location and stratigraphic position within the Snadd and De Geerdalen formations (Fig. 3); sample numbers are in parentheses. All analysed samples contain detrital zircons with U–Pb age ranges overlapping with the age of deposition.

Twenty-eight percent of the zircon grains in the dataset range between 2900 and 635 Ma. The age peaks in this older subset are much smaller than for the younger zircon populations and similar between the different samples. In Figure 4, the Ladinian deposits, irrespective of location, are compared to Carnian – early Norian deposits and sample 11 from West Spitsbergen. Mesoproterozoic ages dominate the pre-635 Ma zircon populations in the Ladinian samples and sample 11. The pre-635 Ma zircon distribution in the Carnian to lower Norian samples contains fewer Mesoproterozoic zircon grains and has a higher proportion of Neoproterozoic grains, as well as the presence of 2000 and 2500 Ma peaks.

Nordkapp Basin samples (1, 2 and 3), from the southern part of the study area, represent both the lowest and the uppermost stratigraphic levels included in this study (Fig. 3, Table 1). The stratigraphically lowest, Ladinian samples (1 and 2) are dominated by Carboniferous (300 Ma) and Ediacaran – Cambrian peaks (540 Ma) (Fig. 3J, K). The uppermost Carnian Nordkapp Basin sample (3) is distinctly different, with a dominant 235 Ma age peak and a scattered distribution containing Ordovician to Triassic-aged zircons with minor Silurian and Carboniferous peaks (Fig. 3A).

Sentralbanken High samples (5, 6, 7 and 8) of lower Carnian age are similar, with major zircon age peaks in the Triassic (235 Ma), Devonian to Permian (300 Ma) and Ordovician to Silurian (425 Ma) (Fig. 3F–I).

Bjarmeland Platform and Svalbard samples (4, 9 and 10) of middle and upper Carnian age have similar Phanerozoic zircon age distributions with a dominant peak in the Triassic (235 Ma), a Devonian to Permian peak (300 Ma) and an Ordovician to Silurian peak (425 Ma) (Fig. 3C–E).

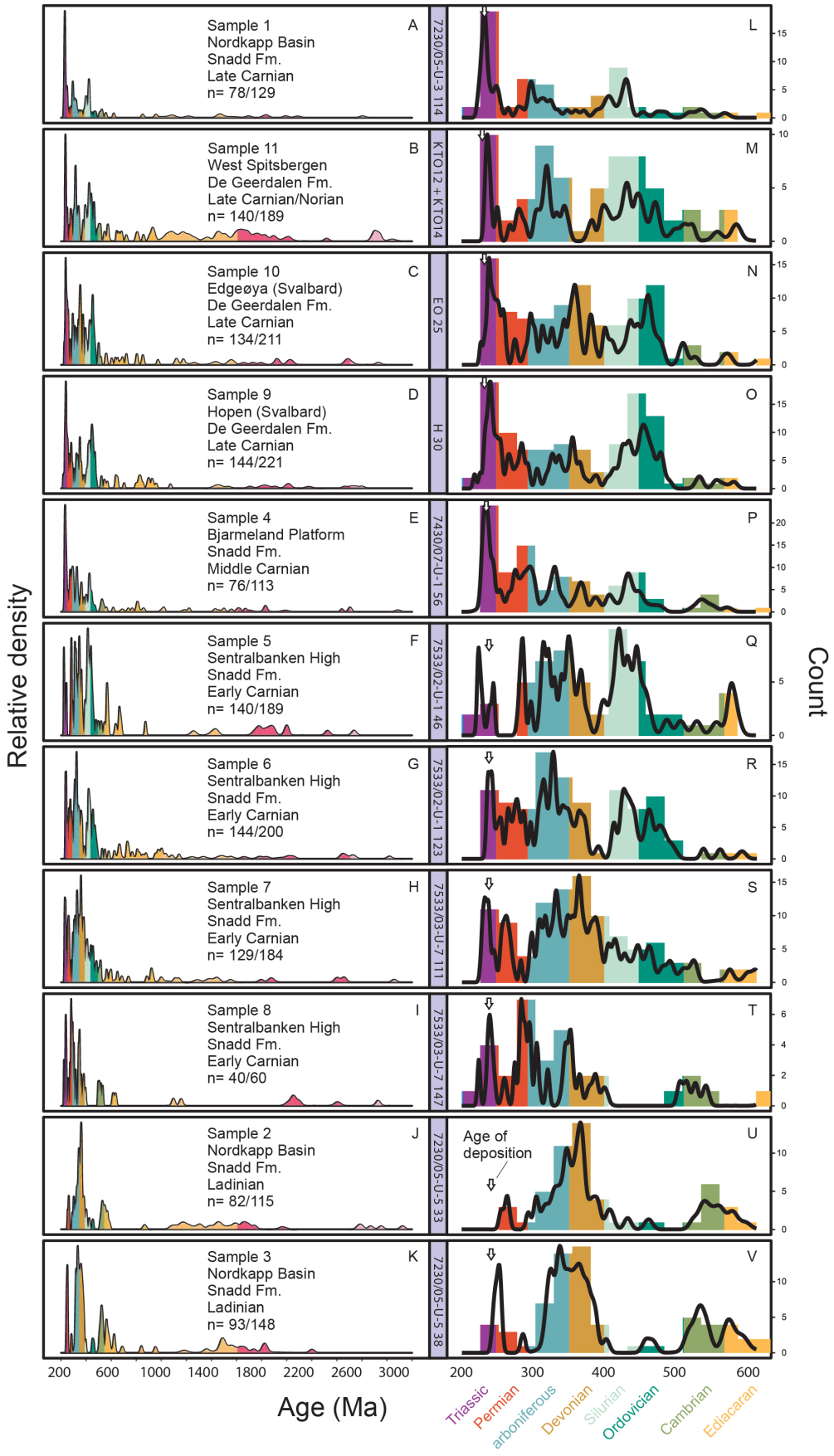

Figure 3. Zircon age distribution diagrams for all samples analysed in this study. The samples are ordered stratigraphically, with the Ladinian samples lowest and early Norian samples at the top. The lowermost samples are dominated by detrital zircons with ages corresponding to the Uralian and Timanian orogens. This distribution is inverted upwards, with just a minor proportion of Carboniferous – Permian grains, and a dominance of Triassic grains in the youngest strata. The only sample with a sizable proportion of Mesoproterozoic and older zircon is located in West Svalbard, indicating a mixed provenance at this location. Arrows denote depositional age.

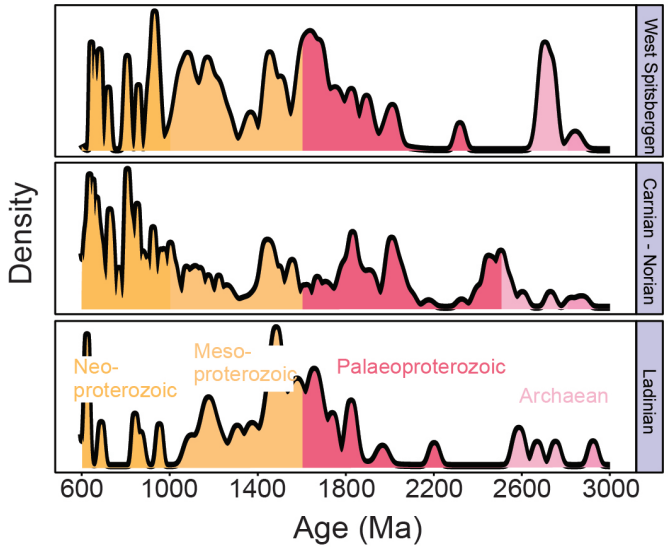

Figure 4. Density-distribution diagrams for the 3000–600 Ma populations of the Ladinian, Carnian – early Norian and West Spitsbergen detrital zircons of this dataset. The Precambrian zircons from West Spitsbergen display patterns similar to earlier Triassic samples (Pózer Bue & Andresen, 2014), and show a mixed provenance area. The Ladinian deposits contain mostly Late Palaeoproterozoic and Mesoproterozoic zircons, but few early Palaeoproterozoic and Neoproterozoic grains. In the Carnian- early Norian deposits, the Mesoproterozoic is less pronounced while Early Palaeoproterozoic and Neoproterozoic zircon ages are prevalent. The observed differences match with observed ages of the Baltica and Siberia cratons, with late Palaeoproterozoic and Mesoproterozoic rocks associated with Baltica (Pózer Bue & Andresen, 2014), and early Palaeoproterozoic and Neoproterozoic rocks found in and around Siberia (Ershova et al., 2016; Priyatkina et al., 2017). However, care must be taken when attempting to identify particular continents based solely on detrital-zircon data (Andersen et al., 2016; Slagstad & Kirkland, 2017)

West Spitsbergen sample (11) of upper Carnian/lowest Norian age is distinctly different from other samples on Svalbard, with a much larger Precambrian zircon age population dominated by Meso-proterozoic and early Neoproterozoic ages (Fig. 3B).

There are four notable Triassic to Ediacaran age groups in the dataset (Fig. 3, right-hand column). A Triassic peak (purple colour) increases in significance stratigraphically upward, from an insignificant peak in the oldest units to a dominant peak in the youngest. Late Devonian to Permian zircon (brown, pale blue and red), corresponding to the age of the Uralian Orogen, is common in all samples but the distribution of ages varies in detail. In the oldest, Ladinian samples, where this age group is the proportionally largest, the predominant age peak is 360 Ma, with Permian ages almost absent. In upper Carnian and lower Norian samples, the proportion of Late Devonian to Permian zircon remains high, although there are fewer Devonian and more Permian zircon grains in the youngest deposits. The Ordovician to Early Devonian (green and pale green) represents a third zircon population present in the Carnian and early Norian samples, with the most prominent age peak at 425 Ma. Zircons with this age are sparse or absent from older, Ladinian samples. A fourth group of Ediacaran to Cambrian ages (orange and olive green), typically associated with the Timanian Orogen, represents a significant peak in Ladinian samples only.

Detrital zircon Lu–Hf isotopic compositions

The investigated detrital-zircon populations display dominantly juvenile (i.e., εHf_t >0, superchondritic) Lu–Hf isotopic compositions (Fig. 5), but with a significant number of subchondritic values. There is no systematic difference between the samples. Archaean and Proterozoic zircon grains have varied but

mostly positive εHf_t values ranging from -10 to +13. Devonian and Carboniferous zircons have εHf_t values mainly between CHUR (chondrite-uniform reservoir) and depleted mantle (DM), indicating juvenile crustal addition or reworking of juvenile crust in the source region(s) in this period. The small number of Hf analyses with corresponding U–Pb discordance <10% for grains younger than c. 300 Ma makes it difficult to say much about the evolution of the youngest source regions. Adopting a more conservative approach in which we define the discordance limit to the closest approach of the 2σ error ellipse to the concordia curve, a larger number of analyses are included. In this case, the samples show a distinct trend towards more negative εHf values, indicative of reworking of older, more isotopically evolved crust.

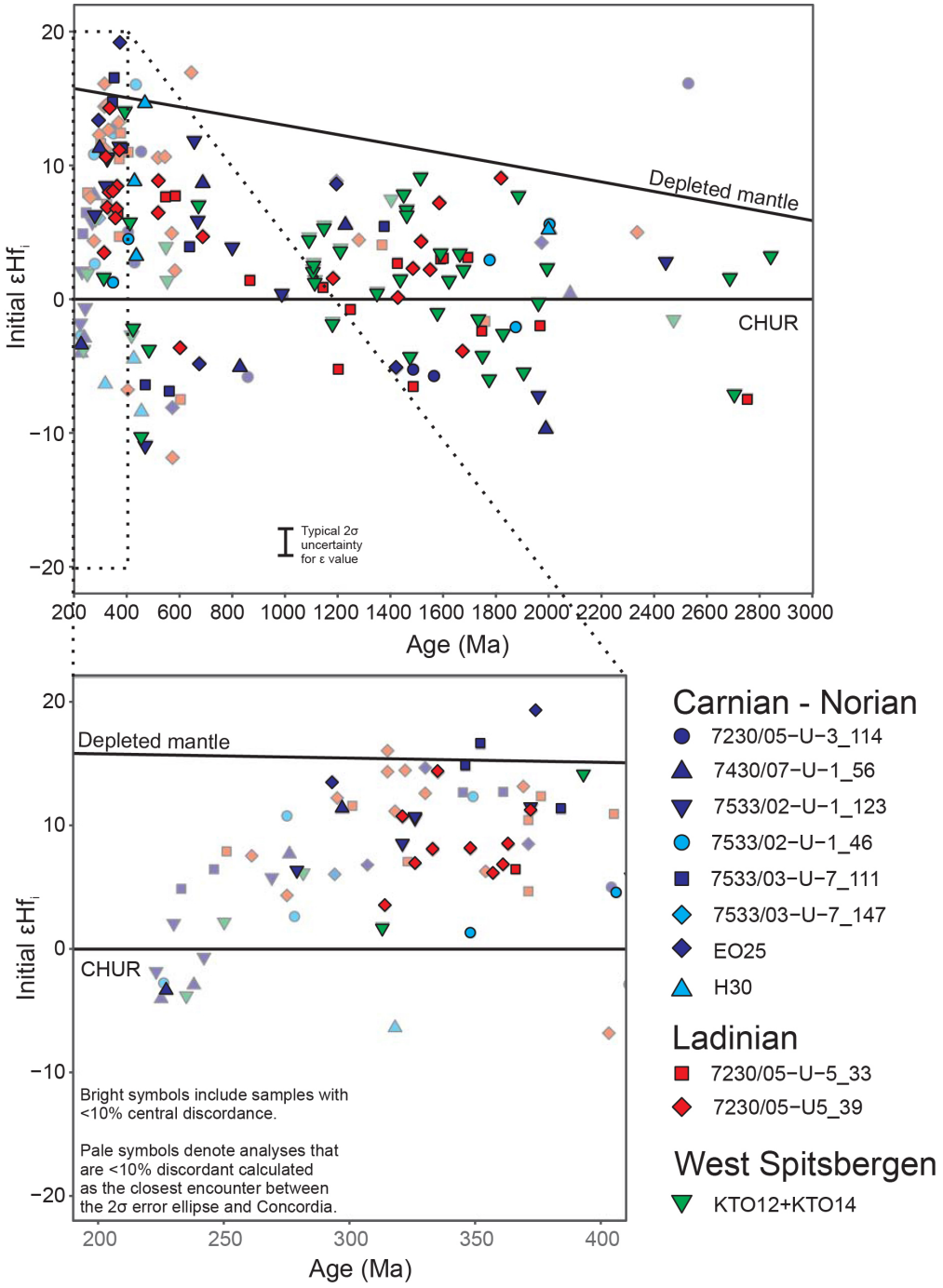

Figure 5. Initial zircon ε_{Hf} vs age plots for the time spans (A) 3000–200 Ma and (B) 400–200 Ma. Phanerozoic zircons display generally mixed juvenile – crustal reworked affinities while Proterozoic zircons mainly have positive ε_{Hf} values. CHUR – chondrite uniform reservoir.

Discussion

Provenance of the Snadd and De Geerdalen formations

The results from our study are broadly in accordance with previous provenance studies of the Snadd and De Geerdalen formations, suggesting a dominant sediment source located southeast of the basin (Mørk, 1999; Riis et al., 2008; Omma et al., 2011; Pózer Bue & Andresen, 2014; Lundschien et al., 2014; Klausen et al., 2015; Soloviev et al., 2015; Fleming et al., 2016; Flowerdew et al., 2019; Khudoley et al., 2019; Harstad et al., 2021). However, the addition of new data from lower Carnian deposits in the Sentralbanken High and lowermost Norian samples from the Nordkapp Basin on the South Barents Shelf allow us to refine this picture, identify and explain temporal variations in source contributions, and discuss geographical variations in source.

Zircon age distributions in the lower strata (Ladinian) of the Snadd Formation, dominated by Uralian and Timanian orogen ages, indicate a provenance associated with the present-day Ural Mountains, where these rock ages are prevalent (Kuznetsov et al., 2007; Puchkov, 2009). However, at some point during the early Carnian, zircons with Triassic, Permian and Ordovician–Silurian ages were introduced alongside mainly Neoproterozoic and Palaeoproterozoic grains (Fig. 3). The region with rock ages and detrital-zircon age populations that best fits with the zircon age spectra present in the Snadd and De Geerdalen formations is the Taimyr Peninsula in northern Siberia and surrounding areas (Letnikova et al., 2014; Ershova et al., 2016; Priyatkina et al., 2017). The 2500, 2000 Ma and Neoproterozoic populations have a clear association with Taimyr and North Siberia but are comparatively uncommon in Baltica and Greenland (Pózer Bue & Andresen, 2014; Ershova et al., 2016; Priyatkina et al., 2017). In Baltica and Laurentia, the Caledonian Orogeny produced zircon of early Palaeozoic age that typically co-occur with Mesoproterozoic zircon ages (Bingen & Solli, 2009).

The link to Taimyr is favoured based on the existence of several Permian to Middle Triassic granitoids related to the South Taimyr Orogen (Kurapov et al., 2021), and the documented Late Triassic volcanism in this region (Fig. 1; Letnikova et al., 2014). Detrital Cr-spinel in the Barents Basin lacks a LIP signature (Harstad et al., 2021), thus a Siberian craton source must be restricted to areas unaffected by Siberian Traps magmatism. It should be noted that the 425 Ma age peak observed in the detrital-zircon dataset remains enigmatic. Based on the available data, the Carnian/Norian strata of the Snadd and De Geerdalen formations appear to have been derived from the Taimyr region, i.e., in contrast to a dominantly Uralian source for the lower, Ladinian strata. The significance of this contrast is discussed further below. The zircon Hf isotope data (Fig. 5) provide additional information relevant to distinguishing provenance. Of particular interest here are the youngest zircon grains, with ages close to the depositional age of the host sediments. The correspondence between detrital-zircon age and age of deposition can be considered an indication of an active, accretionary orogen source (Cawood et al., 2012), or melting of older continental crust by intrusive mafic magma at the onset of extension (Liu et al., 2019), consistent with the range in εHft values from negative (-4) to positive (+8), indicate a mix of juvenile and reworked crustal sources. As shown by Ershova et al. (2018), although Uralian-derived detrital zircons also show considerable spread, they tend to plot at lower εHf values, consistent with the collisional nature of the Uralian Orogen (e.g., Spencer et al., 2019). Reworking of this Uralian crust in the Late Triassic would yield even more evolved Hf compositions, which is not observed in our data. Unfortunately, comparatively few Hf analyses were obtained from the older, Ladinian strata; thus, at the moment we are not able to document that the change in provenance, suggested by changing detrital-zircon ages with stratigraphic position, is also reflected in the Hf data.

Temporal change in source region rather than geographically distinct depositional centres with different sources

The gradual change in detrital-zircon age spectra with younging stratigraphic ages, as suggested by the data presented here, becomes even more prominent when combined with other published data from the Snadd and De Geerdalen formations (Fig. 6, see caption for data sources). Two age peaks (300 and 550 Ma) dominate in the lowest, Ladinian–lower Carnian deposits (Fig. 6D) and gradually decrease in relative size upward in the formations (Fig. 6A–C). In contrast, the 235 and 425 Ma detrital-zircon age peaks are absent or insignificant in the lowermost (Ladinian – lower Carnian) parts of the formations but become dominant in the uppermost (late Carnian - lowest Norian) deposits.

In deposits of uppermost Carnian to lowermost Norian age, the detrital-zircon age distributions in the Sverdrup Basin, on Franz Josef Land and in the Nordkapp Basin (Fig. 7) are dominated by one 235 Ma age peak, indicating the same detrital-zircon source to the entire area. The similarity in detrital-zircon age distributions of sandstone samples located over 1000 km apart (present-day and likely palaeo distance), suggests a high degree of homogeneity in the detritus of this enormous depositional system. It also favours the interpretation of a North Uralian source to the Pat Bay Formation in the eastern Sverdrup Basin (Omma et al., 2011; Hadlari et al., 2018). Considering the Late Triassic sediments of the eastern Sverdrup Basin as a continuation of the already enormous Snadd and De Geerdalen delta (Klausen et al., 2019; Gilmullina et al., 2022) significantly increases the size of the depostional systems. It also explains the Barents basin sediment spill-over documented by Gilmullina et al. (2021), as a continuation into the Sverdrup Basin.

Fleming et al. (2016) were the first to discuss the zircon age variations within the Snadd and De Geerdalen formations and their Franz Joseph Land equivalents. They attributed the observed variations to a difference between the northern and the southern parts of the Uralian Orogen and suggested that the Triassic and Ordovician – Silurian zircons observed in the north better represent Taimyr or north Siberia. The southern samples, on the other hand, were dominated by Devonian – Carboniferous and Ediacaran – Cambrian detrital zircons that can be directly associated with a source in the Uralian and Timanian orogens.

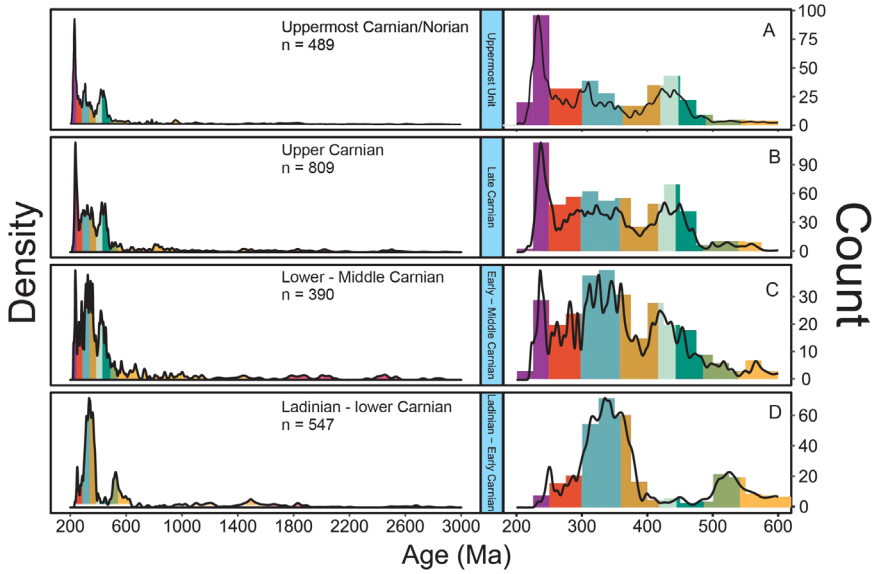

Figure 6. Compilation of all relevant published detrital zircon ages in, or time-equivalent with, the Snadd and De Geerdalen formations, ordered by time of deposition (Omma et al., 2011; Pózer Bue & Andresen, 2014; Soloviev et al., 2015; Fleming et al., 2016; Flowerdew et al., 2019; Khudoley et al., 2019; this study). Complete relative density plots for the time period 3000 – 200 Ma to the left and a focus on the 600 – 200 Ma distributions to the right. We observe a gradual change from a dominant 400 – 300 Ma zircon population in the lowest deposits, through introduction of Triassic and 480–400 Ma zircon grains, with an ultimate dominance of Triassic zircons. The uppermost unit is a composite of samples from the Sverdrup Basin, South Barents Sea and Franz Joseph Land.

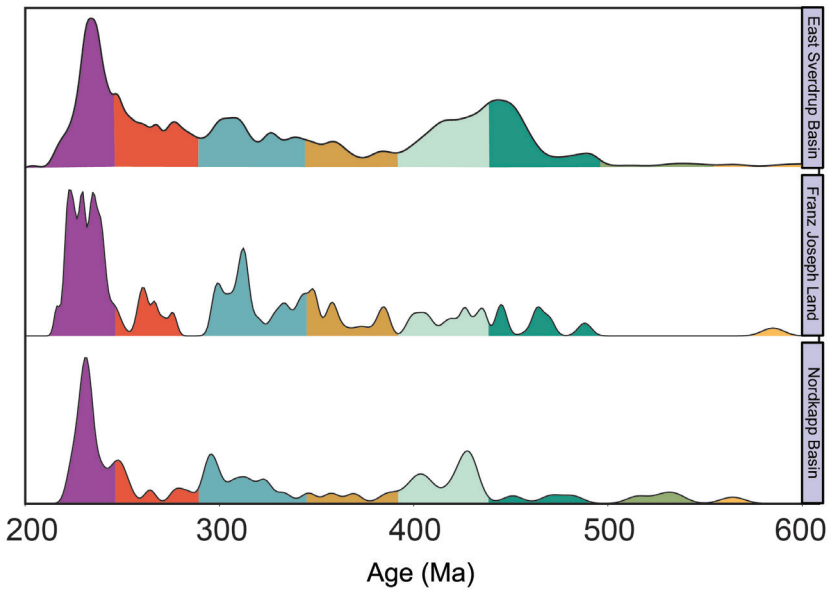

Figure 7. A comparison of detrital-zircon age distributions in samples from the Sverdrup Basin (Omma et al., 2011; Hadlari et al., 2018), the Northeast Barents Shelf (Soloviev et al., 2015) and the Southern Barents Shelf (this study). Samples are of latest Carnian and early Norian age. The similar zircon age distributions demonstrate a similar source to all samples. The eastern parts of the Pat Bay Formation in the Sverdrup Basin can therefore be considered a continuation of the Snadd and De Geerdalen depositional system.

Due to the northwestward migration of clinoforms in the Snadd – De Geerdalen delta (Glørstad-Clark et al., 2010; Klausen et al., 2015, 2019; Gilmullina et al., 2022), there is a rough correlation between geographical location and stratigraphic level within the Snadd Formation and equivalents. When the hypothesis of geographical differences is tested by investigating the top Snadd deposits from a southern location in the Nordkapp Basin, we produced a detrital-zircon age pattern similar to top Snadd equivalents in the far north of the basin. Thus, a hypothesis of consistent geographical differences in zircon age spectra is not supported by the new data (Fig. 7), nor is it supported by previously published detrital Cr-spinel data (Harstad et al., 2021).

Considering the data presented in this and other publications, intra-formational stratigraphic variation and gradual source-terrain evolution/shift represents an alternative interpretation for the observed variations in zircon age spectra, suggesting that temporal changes in source rather than geographical variations are a more likely explanation. Figure 8 shows the evolution in provenance of the Snadd and De Geerdalen formations, as proposed in this contribution. The model involves changes in sediment contribution to relatively stable sediment pathways and is based on the new data presented herein and considerations of the Arctic regional geological evolution, summarised above. The depositional system entered the Barents Basin in the southeast and transported sediments in a northwestward direction, as determined from seismicity-based research (e.g., Klausen et al., 2015). In the Ladinian and early Carnian, the system deposited sediments from the North Uralian and Timanian orogens (Fig. 8A), consistent with a lack of a significant 235 Ma detrital zircon peak. In the early Carnian, however, a younger, 235 Ma component heralds the contribution of a new sediment source, mixed with the Timanian and Uralian orogen sediments. The new source is likely to be in the Taimyr Peninsula (Fig. 8B), where volcanism of this age is known (Letnikova et al., 2014; Kurapov et al., 2021; and references therein). The tectonic explanation for this volcanism, and/or tectonism with concomitant production of considerable sediment volumes in Taimyr in this period cannot be answered based on the data provided in this study. In the middle to late Carnian and earliest Norian, the Taimyr source contributed a progressively larger proportion of detritus (Fig. 8C). The continued contribution from the Uralian Orogen, observed in both detrital zircon and Cr-spinel datasets (Harstad et al., 2021),

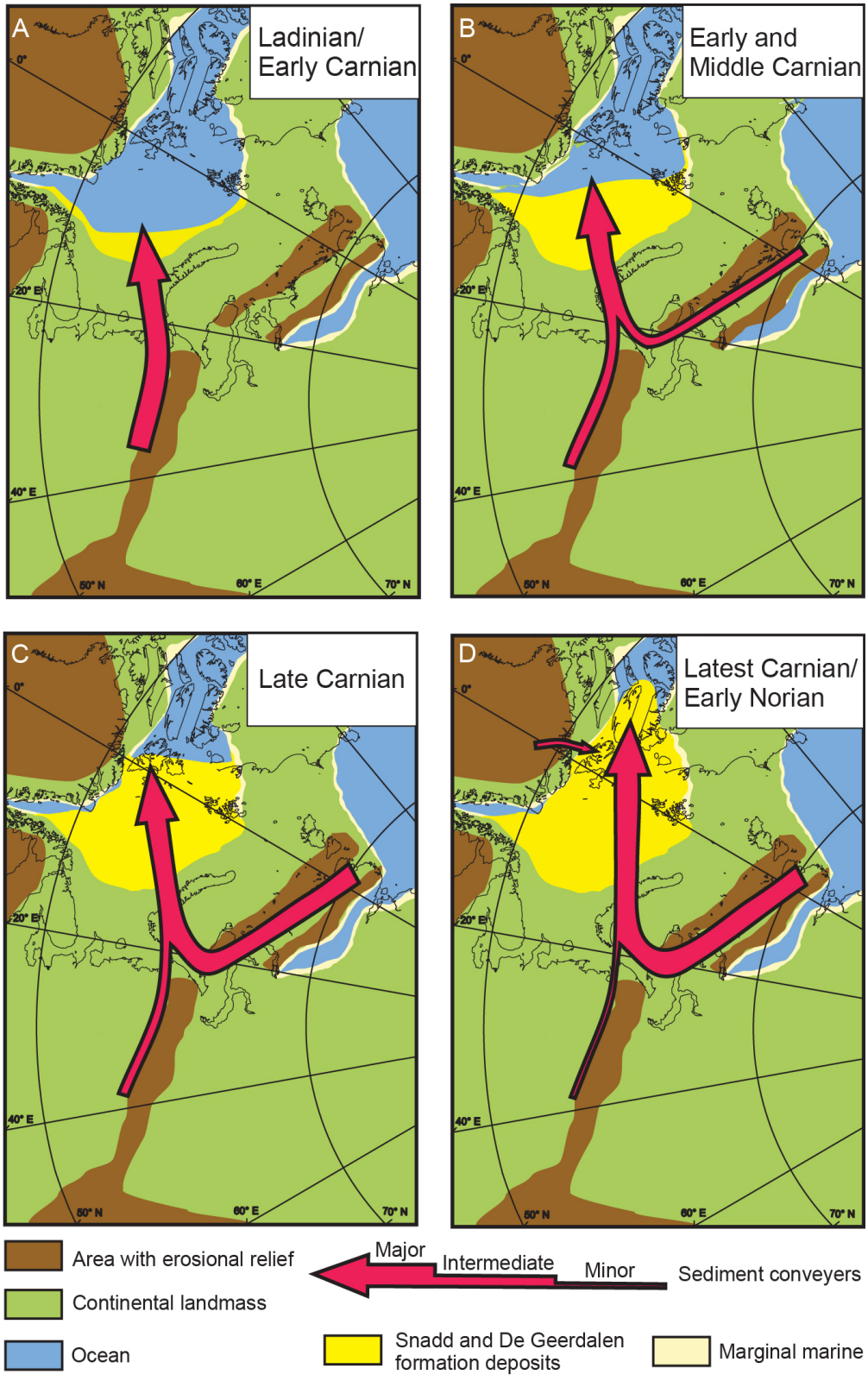

Figure 8. Provenance interpretation and suggested sediment paths into the Barents and Sverdrup palaeobasins for four consecutive Middle – Late Triassic time intervals. (A) The Ladinian and early Carnian detrital-zircon age distributions contain two main age peaks at 300 Ma and 540 Ma, indicating a provenance from the Uralian and Timanian orogens in the north Urals. (B–D) Higher proportions of other detrital zircon populations with ages of 235 and 425 Ma, and reduction in 300 Ma detrital zircon population in the early Carnian to the early Norian suggest gradually increasing input from another source region, likely the Taimyr Peninsula. (D) In late Carnian, a mixed provenance of Greenland and Ural/Taimyr Peninsula is present in West Spitsbergen. The maximum extent of the depositional system was reached in latest Carnian/early Norian and likely extended to include the East Sverdrup Basin. The map is modified from Sømme et al. (2018), with the distribution of the Snadd and De Geerdalen depositional system taken from Klausen et al. (2015) and Anfinson et al. (2016).

suggests that the original supply system did not terminate, but with time grew less significant in terms of sediment delivered (Fig. 8D). It is possible that the youngest zircon grains in the uppermost parts of the formations entered the basin as volcanic ash, expressed as the ~235 Ma age peak. Such an interpretation is supported by the presence of abundant volcanic clasts in the sediments (e.g., Mørk, 1999). The observed increase in two different age-peaks, the 235 Ma and the 425 Ma peaks, combined with the long distance to any known, active volcanic region at the time (the Taimyr Peninsula), favours a significant water-transported contribution to the deposits.

We suggest two analogues to the sedimentary environment discussed above: the present-day Ganges and Brahmaputra drainage system, or the paleo-Mississippi drainage system during the Cenozoic (e.g., Craddock et al., 2013; Blum et al., 2017). In the Ganges-Brahmaputra analogue, Brahmaputra contributes sediment from behind the highest peaks of the Himalayas, while the Ganges represents mountain chain-parallel transport of sediments. We suggest the interpreted Taimyr source to be like a Brahmaputra that steadily increased its sediment contribution to the combined system. The Ganges, on the other hand, is suggested as an analogue to the river draining the remnants of the Uralian and Timanian orogens. Studies of Cenozoic sediments in the Gulf-of Mexico (Craddock et al., 2013; Blum et al., 2017) reveal variations in the relative abundance of detrital zircon ages, interpreted to represent variations in the catchment-area of the paleo-Mississippi, a development highly comparable to what we propose for the Snadd and De Geerdalen drainage system.

Early Norian development on the basin fringes

Sample 11, from the late Carnian/early Norian De Geerdalen formation in Kapp Toscana, West Spitsbergen, has a different detrital-zircon age distribution compared with the other samples in this study. Although the West-Spitsbergen sample has a 500–200 Ma zircon age distribution that is similar to other De Geerdalen-formation samples, the 3000–500 Ma distribution is similar to Early and Middle Triassic sediments derived from the west, most likely from Greenland (Pózer Bue & Andresen, 2014). This distribution is likely the result of mixing of two sediment sources, one representing a continuation of the Middle Triassic Greenland-derived depositional system (Pózer Bue & Andresen, 2014), and the other a Uralian source, similar to that of the Snadd and De Geerdalen formations, farther southeast. Westerly derived sediments have been documented in this area previously (Mørk et al., 1982; Glørstad-Clark et al., 2010), while Harstad et al. (2021) concluded that the Cr-spinel composition in these sediments is similar to that of the Snadd and De Geerdalen formation samples, suggesting little mafic input from western Greenland sources.

Conclusions

The detrital-zircon U–Pb and Lu–Hf data presented here from Ladinian to Norian deposits of the Snadd and De Geerdalen formations on the Barents Shelf are consistent with previous studies arguing for Uralian and Timanian sources. In contrast to previous studies, we show that there is a basin-wide temporal change in provenance, consistent with an initial Uralian source that was gradually replaced by another, Taimyr Peninsula source, which produced zircon similar to the age of deposition.

The prograding depositional system likely reached the Sverdrup Basin in the middle or late Carnian while in West Svalbard, a second minor source region, likely Greenland, is documented in a mixed Greenland and Uralian/Taimyr detrital zircon population.

This study shows the potential for correlation of units over vast distances on the Barents Shelf, identification of particular stratigraphic levels, and acquiring information about the tectonic evolution of source regions reflected in temporally varying sedimentary input.

Our new data suggest a temporal change in source region associated with a gradual change in dominant zircon age peaks from Ladinian (bottom) to Norian (top) deposits. With the new data, top Snadd Formation zircon age distributions are shown to contain remarkably similar detrital-zircon age distributions over a vast area from the Nordkapp Basin in the south Barents Sea to the eastern Sverdrup Basin. A new local source to western Svalbard in the late Carnian is also documented.

The source to the detrital-zircon grains in the Ladinian and lower Carnian deposits of the Snadd Formation is likely Uralian and Timanian orogen rocks in the present-day North Urals. The other progressively more important detrital-zircon source is likely to have been the palaeo-Taimyr area undergoing active tectonism and volcanism at the time. In the Snadd and De Geerdalen formations, we observe a gradual change in detrital-zircon age spectra distribution. This change is characterised by systematic variation in detrital-zircon age-peak distributions. In the oldest deposits, there are two dominant age peaks at 300 Ma and 540 Ma, that gradually change into one dominant 235 Ma age peak and two minor age peaks at 300 Ma and 425 Ma in the youngest deposits. We interpret the change in zircon age distribution to be caused by the introduction and progressive increase of a new, and eventually dominant, zircon source region.

Acknowledgements. We would like to thank our reviewer Michael A. Pointon and an anonymous reviewer for their comments and opinions, which significantly improved the text and figures of this article.

References

Andersen, T., Kristoffersen, M. & Elburg, M.A. 2018: Visualizing, Interpreting and Comparing Detrital Zircon Age and Hf Isotope Data in Basin Analysis–a Graphical Approach. *Basin Research 30*, 132¬–147. https://doi.org/10.1111/bre.12245

Andersen, T., Kristoffersen, M. & Elburg, M.A. 2016. How far can we trust provenance and crustal evolution information from detrital zircons? A South African case study. *Gondwana Research 34*, 129–148. https://doi.org/10.1016/j.gr.2016.03.003

Anfinson, O.A., Embry, A.F. & Stockli, D.F. 2016: Geochronologic Constraints on the Permian–Triassic Northern Source Region of the Sverdrup Basin, Canadian Arctic Islands. *Tectonophysics 691,* pp. 206–219. https://doi.org/10.1016/j.tecto.2016.02.041

Bergan, M. & Knarud, R. 1993: Apparent Changes in Clastic Mineralogy of the Triassic–Jurassic Succession, Norwegian Barents Sea: Possible Implications for Palaeodrainage and Subsidence. *Norwegian Petroleum Society Special Publications 2,* pp. 481–493.
https://doi.org/10.1016/B978-0-444-88943-0.50034-4

Bingen, B. & Solli, A. 2009: Geochronology of Magmatism in the Caledonian and Sveconorwegian Belts of Baltica: Synopsis for Detrital Zircon Provenance Studies. *Norwegian Journal of Geology 89*, pp. 267–290

Black, L.P., Kamo, S.L., Allen, C.M., Aleinikoff, J.N., Davis, D.W., Korsch, R.J. & Foudoulis, C. 2003: Temora 1: A New Zircon Standard for Phanerozoic U–Pb Geochronology. *Chemical geology 200,* pp. 155–170. https://doi.org/10.1016/S0009-2541(03)00165-7

Bugge, T., Elvebakk, G., Fanavoll, S., Mangerud, G., Smelror, M., Weiss, H.M., Gjelberg, J., Kristensen, S.E. & Nilsen, K. 2002: Shallow Stratigraphic Drilling Applied in Hydrocarbon Exploration of the Nordkapp Basin, Barents Sea. *Marine and Petroleum Geology 19*, pp. 13–37. https://doi.org/10.1016/S0264-8172(01)00051-4

Blum, M.D., Milliken, K.T., Pecha, M.A., Snedden, J.W., Frederick, B.C. & Galloway, W.E. 2017: Detrital-zircon records of Cenomanian, Paleocene, and Oligocene Gulf of Mexico drainage integration and sediment routing: Implications for scales of basin-floor fans. *Geosphere 13,* pp. 2169–2205. https://doi.org/10.1130/GES01410.1

Cawood, P.A., Hawkesworth, C. & Dhuime, B. 2012: Detrital Zircon Record and Tectonic Setting. *Geology 40*, pp. 875–878. https://doi.org/10.1130/G32945.1

Cocks, L.R.M. & Torsvik, T.H. 2007: Siberia, the Wandering Northern Terrane, and Its Changing Geography through the Palaeozoic. *Earth-Science Reviews 82*, pp. 29–74. https://doi.org/10.1016/j.earscirev.2007.02.001

Cocks, L.R.M. & Torsvik, T.H. 2011: The Palaeozoic Geography of Laurentia and Western Laurussia: A Stable Craton with Mobile Margins. *Earth-Science Reviews 106,* pp. 1–51. https://doi.org/10.1016/j.earscirev.2011.01.007

Corfu, F., Andersen, T. & Gasser, D. 2014: The Scandinavian Caledonides: Main Features, Conceptual Advances and Critical Questions. Geological Society, London, *Special Publications 390,* pp. 9–43. https://doi.org/10.1144/SP390.25

Craddock, W.H. & Kylander-Clark, A.R. 2013: U–Pb ages of detrital zircons from the Tertiary Mississippi River Delta in central Louisiana: Insights into sediment provenance. *Geosphere 9*, pp. 1832–1851. https://doi.org/10.1130/GES00917.1

Dineley, D. 1975: North Atlantic Old Red Sandstone—Some Implications for Devonian Paleogeography. *Canada's Continental Margins and Offshore Petroleum Exploration 4*, pp. 773–790.

Eide, C.H., Klausen, T.G., Katkov, D., Suslova, A.A. & Helland-Hansen, W. 2018: Linking an Early Triassic Delta to Antecedent Topography: Source-to-Sink Study of the Southwestern Barents Sea Margin. *Bulletin 130,* pp. 263–283. https://doi.org/10.1130/B31639.1

Ershova, V., Prokopiev, A., Andersen, T., Khudoley, A., Kullerud, K. & Thomsen, T.B. 2018: U–Pb and Hf Isotope Analysis of Detrital Zircons from Devonian–Permian Strata of Kotel'ny Island New Siberian Islands, Russian Eastern Arctic): Insights into the Middle–Late Paleozoic Evolution of the Arctic. *Journal of Geodynamics 119,* pp. 199–209. https://doi.org/10.1016/j.jog.2018.02.008

Ershova, V.B., Khudoley, A.K., Prokopiev, A.V., Tuchkova, M.I., Fedorov, P.V., Kazakova, G.G., Shishlov, S.B. & O'Sullivan, P. 2016: Trans-Siberian Permian Rivers: A Key to Understanding Arctic Sedimentary Provenance. *Tectonophysics 691*, pp. 220–233. https://doi.org/10.1016/j.tecto.2016.03.028

Fleming, E.J., Flowerdew, M.J., Smyth, H.R., Scott, R.A., Morton, A.C., Omma, J.E., Frei, D. & Whitehouse, M.J. 2016: Provenance of Triassic Sandstones on the Southwest Barents Shelf and the Implication for Sediment Dispersal Patterns in Northwest Pangaea. *Marine and petroleum geology 78*, pp. 516–535. https://doi.org/10.1016/j.marpetgeo.2016.10.005

Flowerdew, M.J., Fleming, E.J., Morton, A.C., Frei, D., Chew, D.M. & Daly, J.S. 2019: Assessing Mineral Fertility and Bias in Sedimentary Provenance Studies: Examples from the Barents Shelf. Geological *Society London Special Publications 484,* SP484. 11. https://doi.org/10.1144/SP484.1

Gee, D.G. & Pease, V. 2004: The Neoproterozoic Timanide Orogen of Eastern Baltica: Introduction. *Geological Society, London, Memoirs 30*, pp. 1–3. https://doi.org/10.1144/GSL.MEM.2004.030.01.01

Gee, D., Bogolepova, O. & Lorenz, H. 2006: The Timanide, Caledonide and Uralide Orogens in the Eurasian High Arctic, and Relationships to the Palaeo-Continents Laurentia, Baltica and Siberia. *Geological Society London Memoirs 32*, pp. 507-520. https://doi.org/10.1144/GSL.MEM.2006.032.01.31

Gilmullina, A., Klausen, T.G., Paterson, N.W., Suslova, A. & Haug Eide, C. 2021: Regional Correlation and Seismic Stratigraphy of Triassic Strata in the Greater Barents Sea: Implications for Sediment Transport in Arctic Basins. *Basin Research.* https://doi.org/10.1111/bre.12526

Gilmullina, A., Klausen, T. G., Doré, A.G., Sirevaag, H., Suslova, A. & Eide, C.H. 2022: Arctic sediment routing during the Triassic-sinking the Arctic Atlantis. *Journal of the Geological Society 180*, jgs2022-018. https://doi.org/10.1144/jgs2022-018

Glørstad-Clark, E., Faleide, J.I., Lundschien, B.A. & Nystuen, J.P. 2010: Triassic Seismic Sequence Stratigraphy and Paleogeography of the Western Barents Sea Area. *Marine and Petroleum Geology 27,* pp. 1448–1475. https://doi.org/10.1016/j.marpetgeo.2010.02.008

Hadlari, T., Dewing, K., Matthews, W. A., Alonso-Torres, D., & Midwinter, D. 2018: Early Triassic development of a foreland basin in the Canadian high Arctic: implications for a Pangean Rim of Fire. *Tectonophysics 736*, pp. 75–84. https://doi.org/10.1016/j.tecto.2018.04.020

Harstad, T.S., Mørk, M.B.E. & Slagstad, T. 2021: The Importance of Trace Element Analyses in Detrital Cr-Spinel Provenance Studies: An Example from the Upper Triassic of the Barents Shelf. *Basin Research 33*, pp. 1017–1032. https://doi.org/10.1111/bre.12502

Henriksen, E., Bjørnseth, H., Hals, T., Heide, T., Kiryukhina, T., Kløvjan, O., Larssen, G., Ryseth, A., Rønning, K. & Sollid, K. 2011: Uplift and Erosion of the Greater Barents Sea: Impact on Prospectivity and Petroleum Systems. *Geological Society London Memoirs 35*, pp. 271–281. https://doi.org/10.1144/M35.17

Høy, T. & Lundschien, B. 2011: Triassic Deltaic Sequences in the Northern Barents Sea. *Geological Society London Memoirs 35*, pp. 249–260. https://doi.org/10.1144/M35.15

Ivanov, A.V., Demonterova, E.I., Savatenkov, V.M., Perepelov, A.B., Ryabov, V.V. & Shevko, A.Y. 2018: Late Triassic Carnian: Lamproites from Noril'sk, Polar Siberia: Evidence for Melting of the Recycled Archean Crust and the Question of Lamproite Source for Some Placer Diamond Deposits of the Siberian Craton. *Lithos 296*, pp. 67–78. https://doi.org/10.1016/j.lithos.2017.10.021

Jackson, S.E., Pearson, N.J., Griffin, W.L. & Belousova, E.A. 2004: The Application of Laser Ablation-Inductively Coupled Plasma-Mass Spectrometry to in situ U–Pb Zircon Geochronology. *Chemical Geology 211*, pp. 47–69. https://doi.org/10.1016/j.chemgeo.2004.06.017

Khudoley, A.K., Verzhbitsky, V.E., Zastrozhnov, D.A., O'Sullivan, P., Ershova, V.B., Proskurnin, V.F., Tuchkova, M.I., Rogov, M.A., Kyser, T.K. & Malyshev, S.V. 2018: Late Paleozoic–Mesozoic Tectonic Evolution of the Eastern Taimyr-Severnaya Zemlya Fold and Thrust Belt and Adjoining Yenisey-Khatanga Depression. *Journal of Geodynamics 119,* pp. 221–241. https://doi.org/10.1016/j.jog.2018.02.002

Khudoley, A.K., Sobolev, N.N., Petrov, E.O., Ershova, V.B., Makariev, A.A., Makarieva, E.V., Gaina, C. & Sobolev, P.O. 2019: A Reconnaissance Provenance Study of Triassic–Jurassic Clastic Rocks of the Russian Barents Sea. *Geologiska Föreningen i Stockholm Förhandlingar,* pp. 1–9. https://doi.org/10.1080/11035897.2019.1621372

Klausen, T.G., Ryseth, A.E., Helland-Hansen, W., Gawthorpe, R. & Laursen, I. 2015: Regional Development and Sequence Stratigraphy of the Middle to Late Triassic Snadd Formation, Norwegian Barents Sea. *Marine Petroleum Geology 62*, pp. 102–122. https://doi.org/10.1016/j.marpetgeo.2015.02.004

Klausen, T.G., Müller, R., Slama, J. & Helland-Hansen, W. 2017: Evidence for Late Triassic Provenance Areas and Early Jurassic Sediment Supply Turnover in the Barents Sea Basin of Northern Pangea. *Lithosphere 9*, pp. 14–28. https://doi.org/10.1130/L556.1

Klausen, T.G., Nyberg, B. & Helland-Hansen, W. 2019: The Largest Delta Plain in Earth's History. *Geology 47*, pp. 470–474. https://doi.org/10.1130/G45507.1

Kurapov, M., Ershova, V., Khudoley, A., Luchitskaya, M., Stockli, D., Makariev, A., Makarieva, E. & Vishnevskaya, I. 2021: Latest Permian–Triassic magmatism of the Taimyr Peninsula: New evidence for a connection to the Siberian Traps large igneous province. *Geosphere 17,* pp. 2062–2077. https://doi.org/10.1130/GES02421.1

Kuznetsov, N., Soboleva, A., Udoratina, O., Hertseva, M. & Andreichev, V. 2007: Pre-Ordovician Tectonic Evolution and Volcano–Plutonic Associations of the Timanides and Northern Pre-Uralides, Northeast Part of the East European Craton. *Gondwana Research 12*, pp. 305–323. https://doi.org/10.1016/j.gr.2006.10.021

Letnikova, E., Izokh, A., Nikolenko, E., Pokhilenko, N., Shelestov, V., Hilen, G. & Lobanov, S. 2014: Late Triassic High-Potassium Trachitic Volcanism of the Northeast of the Siberian Platform: Evidence in the Sedimentary Record. *Doklady Earth Sciences 459,* pp. 1344–1347. https://doi.org/10.1134/S1028334X14110221

Line, L.H., Müller, R., Klausen, T.G., Jahren, J. & Hellevang, H. 2020: Distinct Petrographic Responses to Basin Reorganization across the Triassic–Jurassic Boundary in the Southwestern Barents Sea. *Basin Research*. https://doi.org/10.1111/bre.12437

Liu, H., XU, Y., Zhong, Y., Luo, Z., Mundil, R., Riley, T.R., Zhang, L. & Xie, W. 2019: Crustal melting above a mantle plume: Insights from the Permian Tarim Large Igneous Province, NW China. *Lithos 326*, pp. 326–327. https://doi.org/10.1016/j.lithos.2018.12.031

Lorenz, H., Gee, D.G. & Simonetti, A. 2008: Detrital Zircon Ages and Provenance of the Late Neoproterozoic and Palaeozoic Successions on Severnaya Zemlya, Kara Shelf: A Tie to Baltica. *Norwegian Journal of Geology 88,* pp. 235–258.

Lorenz, H., Gee, D.G., Korago, E., Kovaleva, G., McClelland, W.C., Gilotti, J.A. & Frei, D. 2013: Detrital Zircon Geochronology of Palaeozoic Novaya Zemlya–a Key to Understanding the Basement of the Barents Shelf. *Terra Nova 25,* pp. 496–503. https://doi.org/10.1111/ter.12064

Lundschien, B.A., Høy, T. & Mørk, A. 2014: Triassic Hydrocarbon Potential in the Northern Barents Sea; Integrating Svalbard and Stratigraphic Core Data. *Norwegian Petroleum Directorate Bulletin 11*, pp. 3–20.

Midwinter, D., Hadlari, T., Davis, W., Dewing, K. & Arnott, R. 2016: Dual Provenance Signatures of the Triassic Northern Laurentian Margin from Detrital-Zircon U–Pb and Hf-Isotope Analysis of Triassic–Jurassic Strata in the Sverdrup Basin. *Lithosphere 8,* pp. 668–683. https://doi.org/10.1130/L517.1

Miller, E.L., Toro, J., Gehrels, G., Amato, J.M., Prokopiev, A., Tuchkova, M.I., Akinin, V.V., Dumitru, T.A., Moore, T.E. & Cecile, M.P. 2006: New Insights into Arctic Paleogeography and Tectonics from U-Pb Detrital Zircon Geochronology. *Tectonics 25.* https://doi.org/10.1029/2005TC001830

Miller, E.L., Soloviev, A.V., Prokopiev, A.V., Toro, J., Harris, D., Kuzmichev, A.B. & Gehrels, G.E. 2013: Triassic River Systems and the Paleo-Pacific Margin of Northwestern Pangea. *Gondwana Research 23*, pp. 1631–1645. https://doi.org/10.1016/j.gr.2012.08.015

Morton, A.C. & Hallsworth, C.R. 1999: Processes Controlling the Composition of Heavy Mineral Assemblages in Sandstones. *Sedimentary Geology 124*, pp. 3–29. https://doi.org/10.1016/S0037-0738(98)00118-3

Müller, A. & Knies, J. 2013: Trace elements and cathodoluminescence of detrital quartz in Arctic marine sediments – a new ice-rafted debris provenance proxy, *Climate of the Past 9*, pp. 2615–2630. https://doi.org/10.5194/cp-9-2615-2013

Mørk, A., Knarud, R. & Worsley, D. 1982: Depositional and Diagenetic Environments of the Triassic and Lower Jurassic Succession of Svalbard. *In* Embry, A.F. & Balkwill, H.R. (eds.): *Arctic Geology and Geophysics*, Canadian Society of Petroleum geology, pp. 371–398.

Mørk, M.B.E. 1999: Compositional Variations and Provenance of Triassic Sandstones from the Barents Shelf. *Journal of Sedimentary Research 69,* pp. 690–710. https://doi.org/10.2110/jsr.69.690

Mørk, M.B.E. 2013: Diagenesis and Quartz Cement Distribution of Low-Permeability Upper Triassic–Middle Jurassic Reservoir Sandstones, Longyearbyen Co2 Lab Well Site in Svalbard, Norway. *AAPG bulletin 97,* pp. 577–596. https://doi.org/10.1306/10031211193

Nikishin, A., Sobornov, K., Prokopiev, A. & Frolov, S. 2010: Tectonic Evolution of the Siberian Platform During the Vendian and Phanerozoic. *Moscow University Geology Bulletin 65*, pp. 1–16. https://doi.org/10.3103/S0145875210010011

Nikolenko, E., Logvinova, A., Izokh, A., Afanas'ev, V., Oleynikov, O. & Biller, A.Y. 2018: Cr-Spinel Assemblage from the Upper Triassic Gritstones of the Northeastern Siberian Platform. *Russian Geology and Geophysics 59,* pp. 1348–1364. https://doi.org/10.1016/j.rgg.2018.09.011

Nystuen, J.P., Andresen, A., Kumpulainen, R.A. & Siedlecka, A. 2008: Neoproterozoic Basin Evolution in Fennoscandia, East Greenland and Svalbard. *Episodes 31*, pp. 35–43. https://doi.org/10.18814/epiiugs/2008/v31i1/006

Olovyanishnikov, V.G., Roberts, D. & Siedlecka, A. 2000: Tectonics and Sedimentation of the Meso-to Neoproterozoic Timan-Varanger Belt Along the Northeastern Margin of Baltica. *Polarforschung 68,* pp. 267–274.

Omma, J., Pease, V. & Scott, R. 2011: U–Pb Sims Zircon Geochronology of Triassic and Jurassic Sandstones on Northwestern Axel Heiberg Island, Northern Sverdrup Basin, Arctic Canada. *Geological Society London Memoirs 35*, pp. 559–566. https://doi.org/10.1144/M35.37

Patchett, P. J. & Tatsumoto, M. 1980: Hafnium isotope variations in oceanic basalts. *Geophysical Research Letters 7*, pp. 1077–1080. https://doi.org/10.1029/GL007i012p01077

Priyatkina, N., Collins, W.J., Khudoley, A., Zastrozhnov, D., Ershova, V., Chamberlain, K., Shatsillo, A. & Proskurnin, V. 2017: The Proterozoic Evolution of Northern Siberian Craton Margin: A Comparison of U–Pb–Hf Signatures from Sedimentary Units of the Taimyr Orogenic Belt and the Siberian Platform. *International Geology Review 59,* pp. 1632–1656. https://doi.org/10.1080/00206814.2017.1289341

Pozer Bue, E. & Andresen, A. 2014: Constraining Depositional Models in the Barents Sea Region Using Detrital Zircon U–Pb Data from Mesozoic Sediments in Svalbard. *Geological Society London Special Publications 386*, pp. 261–279. https://doi.org/10.1144/SP386.14

Puchkov, V.N. 2009: The Evolution of the Uralian Orogen. *Geological Society London Special Publications 327*, pp. 161–195. https://doi.org/10.1144/SP327.9

Reichow, M.K., Pringle, M., Al'Mukhamedov, A., Allen, M., Andreichev, V., Buslov, M., Davies, C., Fedoseev, G., Fitton, J. & Inger, S. 2009: The Timing and Extent of the Eruption of the Siberian Traps Large Igneous Province: Implications for the End-Permian Environmental Crisis. *Earth and Planetary Science Letters 277*, 9–20. https://doi.org/10.1016/j.earscirev.2014.08.018

Riis, F., Lundschien, B.A., Høy, T., Mørk, A. & Mørk, M.B.E. 2008: Evolution of the Triassic Shelf in the Northern Barents Sea Region. *Polar Research 27*, pp. 318–338. https://doi.org/10.1111/j.1751-8369.2008.00086.x

Skår, Ø. 2002: U–Pb Geochronology and Geochemistry of Early Proterozoic Rocks of the Tectonic Basement Windows in Central Nordland, Caledonides of North-Central Norway. *Precambrian Research 116,* pp. 265–283. https://doi.org/10.1016/S0301-9268(02)00026-8

Slagstad, T. & Kirkland, C.L. 2017. The use of detrital zircon data in terrane analysis: A nonunique answer to provenance and tectonostratigraphic position in the Scandinavian Caledonides. Lithosphere 9, pp. 1002–1011. https://doi.org/10.1130/L663.1

Sláma, J., Košler, J., Condon, D.J., Crowley, J.L., Gerdes, A., Hanchar, J.M., Horstwood, M.S., Morris, G.A., Nasdala, L. & Norberg, N. 2008: Plešovice Zircon—a New Natural Reference Material for U–Pb and Hf Isotopic Microanalysis. *Chemical Geology 249*, pp. 1–35. https://doi.org/10.1016/j.chemgeo.2007.11.005

Soloviev, A., Zaionchek, A., Suprunenko, O., Brekke, H., Faleide, J., Rozhkova, D., Khisamutdinova, A., Stolbov, N. & Hourigan, J. 2015: Evolution of the Provenances of Triassic Rocks in Franz Josef Land: U/Pb La-Icp-Ms Dating of the Detrital Zircon from Well Severnaya. *Lithology Mineral Resources 50*, pp. 102–116. https://doi.org/10.1134/S0024490215020054

Spencer, C., Kirkland, C., Prave, A., Strachan, R. & Pease, V. 2019: Crustal Reworking and Orogenic Styles Inferred from Zircon Hf Isotopes: Proterozoic Examples from the North Atlantic Region. *Geoscience Frontiers 10,* pp. 417–424. https://doi.org/10.1016/j.gsf.2018.09.008

Stensland, H., Auset, M., Elvebakk, G. & Mørk, M.B.E. 2013: Palaeosols and Eogenesis of Triassic Sediments from Shallow Cores at the Bjarmeland Platform and in the Nordkapp Basin, Southwestern Barents Sea. *Abstract and Poster, Norsk Geologisk Forenings Landsmøte, Oslo, 8th-10th of January 2013.*

Sømme, T., Doré, A., Lundin, E. & Tørudbakken, B. 2018: Triassic–Paleogene Paleogeography of the Arctic: Implications for Sediment Routing and Basin Fill. *AAPG Bulletin 102*, pp. 2481–2517. https://doi.org/10.1306/05111817254

Tuchkova, M., Sokolov, S., Khudoley, A., Verzhbitsky, V., Hayasaka, Y. & Moiseev, A. 2011: *Permian and Triassic Deposits of Siberian and Chukotka Passive Margins: Sedimentation Setting and Provenances. ICAM VI: Proceedings of the International Conference on Arctic Margins VI, Fairbanks, Alaska.*

Van Actherbergh, E. 2001: Data Reduction Software for La-Icp-Ms. *Laser Ablation-ICP-mass spectrometry in the earth sciences: principles and applications,* pp. 239–243.

Vernikovsky, V.A., Vernikovskaya, A., Proskurnin, V., Matushkin, N., Proskurnina, M., Kadilnikov, P., Larionov, A. & Travin, A. 2020: Late Paleozoic–Early Mesozoic Granite Magmatism on the Arctic Margin of the Siberian Craton During the Kara-Siberia Oblique Collision and Plume Events. *Minerals 10,* 571. https://doi.org/10.3390/min10060571

Vigran, J.O., Mangerud, G., Mørk, A. & Hochuli, P.A. 2014: Palynology and Geology of the Triassic Succession of Svalbard and the Barents Sea. *Geological Survey of Norway Special Publication 14,* 270.

Wiedenbeck, M., Alle, P., Corfu, F., Griffin, W., Meier, M., Oberli, F., von Quadt, A., Roddick, J. & Spiegel, W. 1995: Three Natural Zircon Standards for U–Th–Pb, Lu–Hf, Trace Element and Ree Analyses. *Geostandards newsletter 19,* pp. 1–23. https://doi.org/10.1111/j.1751-908X.1995.tb00147.x

Willner, A.P., Gopon, M., Glodny, J., Puchkov, V.N. & Schertl, H.-P. 2019: Timanide Ediacaran-Early Cambrian: Metamorphism at the Transition from Eclogite to Amphibolite Facies in the Beloretsk Complex, Sw-Urals, Russia. *Journal of Earth Science 30*, pp. 1144–1165. https://doi.org/10.1007/s12583-019-1249-2

Woodhead, J., Hergt, J., Shelley, M., Eggins, S. & Kemp, R. 2004: Zircon Hf-Isotope Analysis with an Excimer Laser, Depth Profiling, Ablation of Complex Geometries, and Concomitant Age Estimation. *Chemical Geology 209,* pp. 121–135. https://doi.org/10.1016/j.chemgeo.2004.04.026

Xiao, W., Windley, B.F., Sun, S., Li, J., Huang, B., Han, C., Yuan, C., Sun, M. & Chen, H. 2015: A Tale of Amalgamation of Three Permo-Triassic Collage Systems in Central Asia: Oroclines, Sutures, and Terminal Accretion. *Annual Review of Earth and Planetary Sciences 43*, pp. 477–507. https://doi.org/10.1146/annurev-earth-060614-105254

Zhang, X., Pease, V., Skogseid, J. & Wohlgemuth-Ueberwasser, C. 2016: Reconstruction of Tectonic Events on the Northern Eurasia Margin of the Arctic, from U-Pb Detrital Zircon Provenance Investigations of Late Paleozoic to Mesozoic Sandstones in Southern Taimyr Peninsula. *Bulletin 128,* pp. 29–46. https://doi.org/10.1130/B31241.1

Zhang, X., Pease, V., Carter, A., Kostuychenko, S., Suleymanov, A. & Scott, R. 2018a: Timing of Exhumation and Deformation across the Taimyr Fold–Thrust Belt: Insights from Apatite Fission Track Dating and Balanced Cross-Sections. *Geological Society London Special Publications 460,* pp. 315–333. https://doi.org/10.1144/SP460.3

Zhang, X., Pease, V., Carter, A. & Scott, R. 2018b: Reconstructing Palaeozoic and Mesozoic Tectonic Evolution of Novaya Zemlya: Combing Geochronology and Thermochronology. *Geological Society London Special Publications 460,* pp. 335–353. https://doi.org/10.1144/SP460.13